Integrated Modeling for the VLTI

Michael Müller[a], Rainer Wilhelm[b], Horst Baier[a] and Bertrand Koehler[b]

[a] Institute of Lightweight Structures (LLB), Technische Universität München
[b]European Southern Observatory (ESO)

D-85748 Garching b. München, Germany

ABSTRACT

Within the scope of the Very Large Telescope Interferometer (VLTI) project, a set of software tools for integrated modeling of ground- and space-based stellar interferometers has been developed. Integrated modeling aims at time-dependent system analysis combining different technical disciplines (optics, mechanical structure, control system with sensors and actuators, environmental disturbances). The main components of the software are **BeamWarrior**, a tool for creation of dynamic optical models, and **SMI** (Structural Modeling Interface), which generates linear state-space models from finite element models of a mechanical structure. Based on these tools, models of the various subsystems (e.g. telescope, delay line, beam combiner) can be created in the relevant technical disciplines (e.g. optics, structure). All subsystem models are integrated into the Matlab/Simulink environment for dynamic control system simulations. The output of the dynamic model is a complete description of the time-dependent electromagnetic field in each interferometer arm. This output serves as input to an instrument model simulating the creation of interference fringes.

This paper shows the application of the integrated modeling concept to the VLTI. The architecture of a Simulink-based integrated model with its main components, telescope structures, optics and control loops, is presented. Disturbance models for wind load, seismic ground excitation and atmospheric turbulence are included. Beam combination is performed using a simplified model of the VINCI instrument. Results of closed-loop dynamic simulations are presented.

Keywords: integrated modeling, optical modeling, telescope structures, finite element modeling, stellar interferometry, VLTI, VINCI

1. INTRODUCTION

Research and development in the field of optical stellar interferometry combines several engineering disciplines such as actively controlled optics, structural mechanics, thermodynamics and control engineering. Interactions between the subsystems of a stellar interferometer are subject to various disturbances. Ground-based interferometers such as the VLTI are particularly subject to environmental disturbances such as wind load, seismic excitation and atmospheric turbulence, whereas spaceborne systems suffer from pointing errors and optical path-length fluctuations induced by their Guidance, Navigation and Control (GN&C) system. Integrated modeling is a numerical simulation technique for time-dependent system analysis combining different technical disciplines and disturbances. This does *not* include the subsystem design which is performed using specialized tools established in the respective disciplines (e.g. optical design and optimization software, control system identification software, structural Finite Element Method (FEM) software). Based on the detailed design of the subsystems simplified models of those are generated in the respective disciplines (e.g. optics, structure) and then integrated into a dynamic simulation environment. Typical applications of integrated modeling are feasibility assessment, design refinement and performance prediction.

This article presents the architecture and first results of an integrated model for the VLTI. The core of the model is a time-domain simulation of the main VLTI control loops (fringe tracking, fast tip/tilt compensation) implemented in Matlab/Simulink. In contrast to an earlier version of a "VLTI End-to-End Model" used during

Further author information:
Michael Müller: E-mail: mueller@llb.mw.tu-muenchen.de

the VLTI design phase,[1] the current version is based on a modular approach for integrated modeling which can be applied to a wide variety of single- and multi-aperture optical telescopes. Aiming at maximum flexibility and broad applicability, we have developed the software tools **BeamWarrior** and **SMI** (Structural Modeling Interface). They are responsible for generating dynamic models of technical subsystems (e.g. telescope, delay line) in the optical and mechanical disciplines, respectively. The resulting subsystem models are designed for integration into the Simulink environment. In addition to its greater flexibility, the new approach also offers significantly extended capabilities in the areas of optical and mechanical modeling.

Section 2 summarizes the features of **BeamWarrior** and **SMI**. Section 3 describes the architecture of the VLTI integrated model. Results of dynamic simulations are shown. The article ends with a summary and an outlook to future work in Section 4

2. THE SOFTWARE TOOLS

2.1. The optical modeling tool BeamWarrior

BeamWarrior is a tool to generate models of the optical signal flow influenced by perturbations. Its development was initiated in 1997, driven by the lack of powerful, open-architecture optical modeling code which could easily be customized to create models for integration into a control loop simulation. The institutions which have supported the development are Astrium GmbH, ESO and the German Aerospace Center (DLR). Present and future work is done in an ESO-Astrium team. In the framework of an ESA Technology Research Programme (TRP), **BeamWarrior** is used to develop an integrated model (FINCH) of the spaceborne nulling interferometry mission *Darwin*.

The **BeamWarrior** *Kernel* is a library of ANSI C functions for optical modeling which can be accessed either by a custom C application or via the **BeamWarrior** *Optical Modeling Tool*. The latter is a general-purpose application which reads a sequence of computational steps to be performed and the results to be produced from an ASCII "control file". The *Optical Modeling Tool* has been designed for flexible generation of linear optical models (i.e. sensitivity matrices). Besides its main purpose, namely the creation of dynamic optical models, **BeamWarrior** can also be employed for a large variety of static optical analysis tasks. Examples can be found in the references.

Light propagation is simulated by geometrical- or wave-optical methods which can be flexibly combined in a "hybrid propagation model". The geometrical-optical domain is covered by a radiometric polarization ray tracing algorithm. Wave-optical (diffraction) propagation is handled by three alternative approaches, each being suitable for specific cases: (1) the "direct method" based on numerical approximation of the Rayleigh-Sommerfeld integral, (2) the "angular spectrum method" using a decomposition of the optical field into a set of homogeneous and evanescent plane waves, and (3) the powerful Gaussian beam decomposition technique which can be used to simulate an "end-to-end" wave optical propagation —from the incident wavefront to the detector. All Kernel algorithms consider polarization effects and are radiometrically calibrated. A description of the algorithms can be found in the references.[2,3]

Figure 1 shows the spatial distribution of electric field amplitude and phase in the nominal exit pupil plane of a VLTI interferometer arm. As explained later, this result is used in the integrated model.

2.2. The Structural Modeling Interface SMI

For the generation of dynamic mechanical models, LLB has developed the tool **SMI**.[4] It is a Matlab-based software package, which uses modal data from an FEM-analysis and builds a linear time-invariant state-space model of a structure to be used within a time-dependent simulation in the Matlab/Simulink environment. Mechanical models created with **SMI** can easily be coupled to optical models created with **BeamWarrior**. However, the tool can also be used stand-alone.

The basic software architecture is shown in Figure 2. To build a model **SMI** requires modal data from an FEM-analysis. For the FEM software ANSYS an interface for directly loading binary result data is provided. For other FEM packages, this data can also be loaded in a general format.

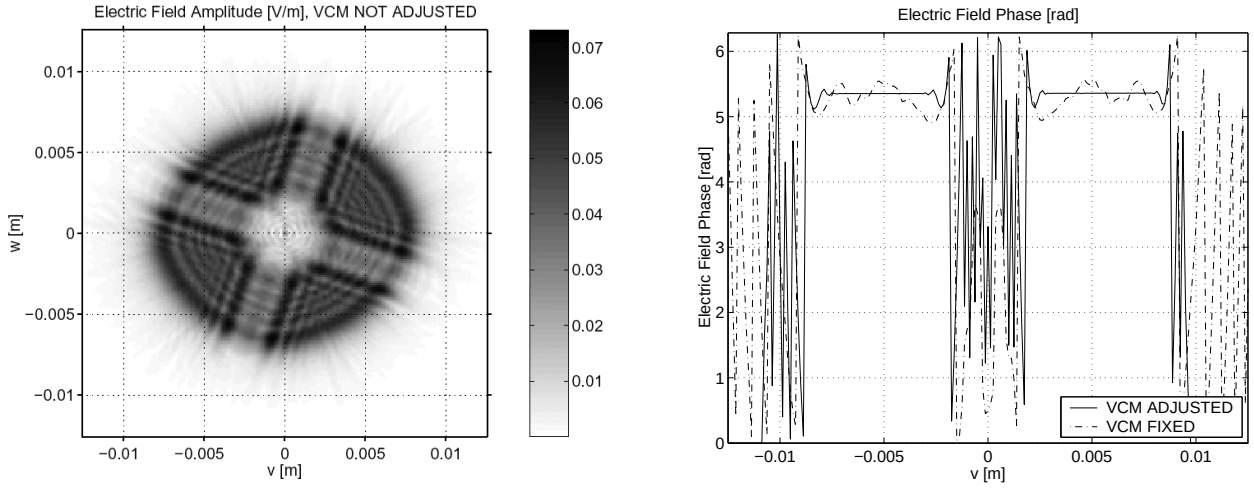

Figure 1. Amplitude (left) and phase (right) of the electric field distribution in the nominal exit pupil (parallel to (v, w)-plane, diameter 18 mm) of a VLTI interferometer arm (Siderostat telescope, $\lambda = 2.2$, point source magnitude $m_K = -6$); shown are amplitude [Vm^{-1}] and phase [rad] of a single Cartesian component polarized along the v-axis (for one linear polarization component of the stellar wavefront). The phase distribution is shown along one dimension (v) only. The field distribution was computed assuming a fixed radius of the Variable Curvature Mirror (VCM) inside the VLTI Delay Line (DL), i.e. without active pupil re-imaging ("VCM NOT ADJUSTED (FIXED)"). For comparison, the phase distribution which would be obtained for a correct pupil re-imaging ("VCM ADJUSTED") is also shown.

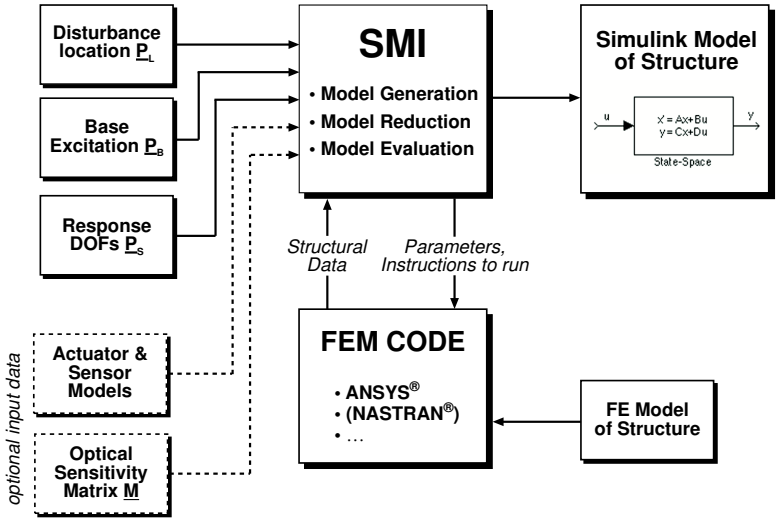

Figure 2. Architecture of **SMI**

To define the system inputs and outputs, the degrees of freedom (DOF) for loads (P_L, P_B) and relevant displacements (P_S) must be defined. A single load can have an arbitrary distribution on the nodes of the FEM structure. The use of different loadsets allows to model loads with mutually independent time-histories (i.e. independent power spectral densities (PSD)). Both force (e.g. wind loads) and base excitation (e.g. ground acceleration due to microseismic perturbations) are supported. The outputs can be combinations of responses of model nodes or the response of a virtual node defined in the FEM model by a constraint equation. Tools are also provided to generate an output representing the best-fit rigid body motion of an elastically deformed

mirror.* **SMI** builds projection matrices to distribute a load onto the individual DOFs of the structure and to get the outputs from the structural deformation. The input/output definition is done using ASCII tables.

With this data **SMI** creates a linear time-invariant state-space model. A key feature of **SMI** is its quality-criteria based tools for manual and automatic model reduction. Individual eigenmodes can be removed manually by the user. Automatic methods are based on effective modal mass tables and balanced truncating. For the balanced truncating the error bounds are displayed. To evaluate the model quality, effective mass tables can be displayed and the transfer functions of full and reduced models can be compared. **SMI** can load an optical sensitivity matrix (linear optical model) $\mathbf{M}$ created by **BeamWarrior**. Moreover, linear models of actuators and sensors can be included. Thus the effect of the model condensation onto the PSD of an output of interest (e.g. the optical path length of a single interferometer arm) for a given input disturbance (e.g. wind force) can be studied.

A clearly structured graphical user interface guides the user through the following steps of generating a dynamic model of the structure: (1) loading the results of a structural analysis (eigenvectors and eigenfrequencies and/or mass and stiffness matrices) produced by an external FEM software (e.g. ANSYS), (2) loading the data for the projection matrices P_L or P_B defining the points of application of input disturbances and loading data for P_S specifying the system outputs, (3) creating a state-space model, (4) reducing the system size while evaluating the model quality and accuracy, and (5) creating a Simulink block representing the dynamic behavior of the structure.

In addition to the above listed features, **SMI** offers the possibility to remotely control ANSYS to perform a modal analysis. If the FE model of the structure is available in a parametrized way, such a remote control could include variations of parameters (e.g. material constants or geometric quantities).

3. INTEGRATED MODELING OF VLTI

In the following, we present the architecture and first results of a recently developed integrated model of the VLTI. The subsystem models assembled in this integrated model were created using the tools described in Sections 2.1 and 2.2. For a system description of the VLTI the reader is referred to *Glindemann et al. 2002.*[5]

3.1. Computing the dynamic interferometer response

The integrated model computes the response of VLTI to a point source (unresolved, infinitely remote) observed on axis. The incident wavefront is an homogeneous (i.e. constant intensity) plane wave. Radiometrically, the source is characterized by its apparent magnitude in a given spectral band (e.g. K-band). Light propagation is simulated for a single wavelength equal to the center wavelength of the spectral band. The point source is assumed to be naturally polarized.

The main output of the model is a complete description of the time-dependent electric field in the exit pupil of each interferometer arm ("time-dependent pupil function"). For computation of the dynamic electric field distributions we use the method described in *Schöller et al. 2000*[1]: The complex electric vector field $\mathbf{E}_i^{Pol}(\mathbf{x},t)$ at the exit pupil of arm i is given by the product of a static complex vector field $\mathbf{E}_i^{Pol}(\mathbf{x})$ and a time-dependent phase factor $\exp(j\Delta\phi_i(\mathbf{x},t)$:

$$\mathbf{E}_i^{Pol}(\mathbf{x},t) = \mathbf{E}_i^{Pol}(\mathbf{x})\exp(j\Delta\phi_i(\mathbf{x},t)) \qquad (Arm\ i, Pol = s,p). \tag{1}$$

where the superscript $Pol = s,p$ denotes the two uncorrelated orthogonal polarization components of the naturally polarized source, t the time and $\mathbf{x} = (v,w)$ a two-dimensional position vector in the exit pupil (compare Figure 1). The dynamic "phase error" $\Delta\phi_i(\mathbf{x},t)$ arises from fluctuations of the optical path in the exit pupil with respect to the static situation. As the displacements of optical elements due to disturbances and active control are sufficiently small the resulting phase error can be regarded as polarization-independent, i.e. the *same* phase factor applies to all Cartesian components of $\mathbf{E}_i^{Pol}$. The phase error is linked to an "optical

*In its current version, **BeamWarrior** only supports conic and cylindrical optical surfaces, i.e. no arbitrarily deformed surfaces.

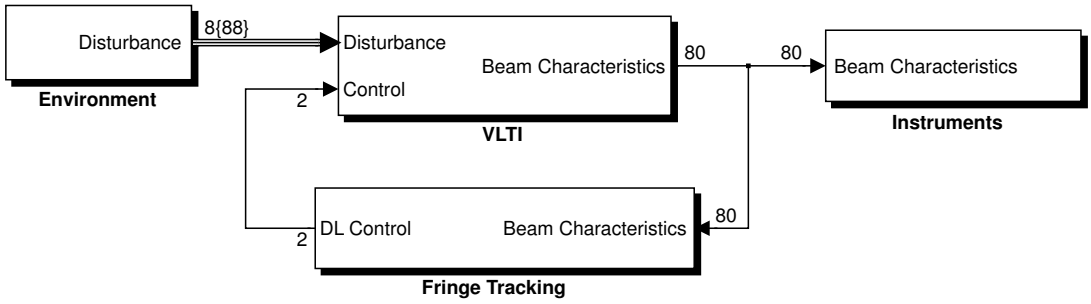

Figure 3. Top-level architecture of the VLTI Integrated Model; the labels attached to the signal flow lines correspond to a two-aperture configuration (see Section 3.2.3).

path error" $\Delta OP(\mathbf{x},t) = \lambda/(2\pi)\Delta\phi_i(\mathbf{x},t)$ which itself can be expressed as decomposition into N orthogonal Zernike polynomials $\psi_m(\mathbf{x})$:

$$\Delta OP(\mathbf{x},t) = \sum_{m=1}^{N} \delta\xi_m(t)\psi_m(\mathbf{x}) \tag{2}$$

The N time-dependent coefficients $\delta\xi_m(t)$ are the deviations of the N Zernike coefficients from the static situation. In addition to dynamic phase errors, the model also takes dynamic pupil motion into account (see Section 3.2.3).

As stated above, the method described computes the response to a point source. However, the formalism can be extended straightforwardly to simulate observation of extended objects (see Schöller et al 2000[1]).

3.2. Model architecture

The architectural design of the VLTI integrated model covers up to eight interferometer arms (in single-feed mode). Each arm is equipped with a "photon collector" (Unit Telescope (UT), Auxiliary Telescope (AT) or Siderostat (SID)) and a DL. The dual-feed mode (PRIMA) is not covered yet. However, the architecture allows a future extension towards it.

Figure 3 shows the top-level architecture of the VLTI integrated model. The model uses a three phased approach: During the *initialization phase*, user-defined parameters are set (e.g. array configuration, source characteristics and angular position, disturbance and control loop parameters, simulation time and sampling). **BeamWarrior** performs the two tasks: (i) compute the static electric vector fields $\mathbf{E}_i^{Pol}(\mathbf{x},t)$ for all interferometer arms ($i = 1 \ldots i_{max}; i_{max} \leq 8$) and both star polarizations ($Pol = s,p$), and (ii) generate the linear optical models (sensitivity matrices) needed for the dynamic simulation.

The *dynamic simulation phase* is the core of the integrated model. It is implemented as a Simulink model. A Simulink block diagram with multiple levels representing the different subsystems is dynamically generated to match the chosen array configuration. The top-most level reflects the fringe tracking control loop as shown in Figure 3.

In the *post-processing phase* the results of the dynamic simulation are combined with the static results obtained in the initialization phase (as described in Section 3.1). A simplified model of the VINCI instrument computes the interference fringes assuming pupil-plane beam combination with a temporal optical pathlength modulation scheme. Alternatively, another instrument model could be used in a future version.

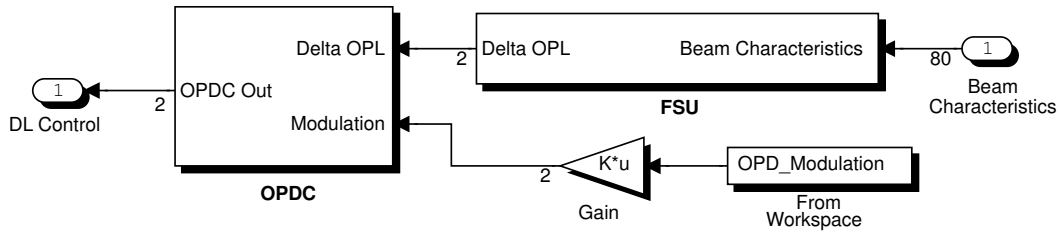

Figure 4. Sensor (FSU) and controller (OPDC) of the fringe tracking control loop; each interferometer arm has its own plant model (Delay Line (DL)) (see Figure 5). The labels attached to the signal flow lines correspond to a two-aperture configuration (see Section 3.2.3).

3.2.1. Control loops

The *fringe tracking control loop* forms the central control loop of the VLTI. It defines the top-layer of the model architecture as shown in Figure 3. The objective of this control loop is to compensate for the (temporarily varying) optical path difference (OPD) between two interferometer arms. Figure 4 depicts the block diagram of the subsystem "`Fringe Tracking`" appearing in Figure 3. The measurement of the OPD is performed by a Fringe Sensor Unit (FSU) located in the beam combination laboratory. The stellar light is shared between FSU and scientific instrument (e.g. VINCI). In general, instrument and FSU operate in different spectral bands. Therefore the light is split by use of dichroic feeding optics. The OPD Controller (OPDC) converts the measured OPD into a command passed to the DL (carriage + Piezo actuator). Optionally, an additional OPD modulation command can be sent in case of pupil plane beam combination. The fringe tracking control loop is present for all three types of photon collectors (UT, AT and SID). Currently, we have implemented a model of the FSU FINITO which will be installed on the VLTI in mid 2003. The DL model is a discrete linear state-space model identified from measurements on site.

For UTs and ATs the *fast tip/tilt loop* compensates for wavefront tip/tilt induced by wind load and atmospheric turbulence. The tip/tilt error is derived from measuring the image position at the transmitted Coudé focus (below the dichroic mirror M9) (see Figure 6). An integrator provides a correction signal to an active mirror (M2 for UT, M6 for AT) which can be actuated in two DOFs (tip/tilt). The tip/tilt control is not available on a SID. Within the model, the image position is computed as spot diagram centroid using a **BeamWarrior** linear optical model for the beam train through the telescope optics (M1...M3), Coudé train (M4...M8) and M9. This *lateral pupil position control loop* (UT and AT only) corrects the lateral position of the exit pupil in the beam combination laboratory. The measurement is taken in the laboratory and fed back to the field mirror M10 which can be actuated in two DOFs (tip/tilt) (see Figure 6). Within the model the lateral pupil position is computed using a **BeamWarrior** linear optical model for the beam train through the whole VLTI optical train up to the instrument entrance (telescope including Coudé train and relay optics, transfer optics, DL, laboratory beam compression/feeding optics). The "real" VLTI does not provide closed-loop control of lateral pupil position (realized by a zero feedback gain in the model). Instead of this, the exit pupil is centered on a CCD matrix by an automatic alignment system before each observation run.

Figure 5 displays the block diagram of a single UT interferometer arm. The signal flows of both tip/tilt loop and lateral pupil position loop are fully contained in the subsystem since these two control loops act independently on each VLTI arm. In contrast, the fringe tracking loop controlling the OPD *between* different arms is implemented on the top-most level of the model. For a description of the signal representations, see Section 3.2.3.

3.2.2. Disturbances

The model considers the following environmental disturbances: wind load, micro-seismic excitation and atmospheric turbulence. Currently wind load and micro-seismic excitation are simulated for UTs only.

The *wind load* acting on the telescope (structure & optics) is modelled using the following approach[4]: Four different load cases are distinguished: (i) primary mirror M1, (ii) M3 mirror and tower, (iii) tube including

center piece and Serrurier bars, and (iv) top unit including M2 housing, spiders and top ring (see Figure 7). For each load case a PSD of the aerodynamic wind force is calculated using an analytical expression based on a von Kármán model. Required parameters such as mean wind speeds, drag coefficients, turbulence intensities, outer scales of turbulence and effective cross-section areas are estimated by "rule-of-thumb calculations" or derived from measurements. The wind force PSDs are converted into random time series. The time series describing the dynamic forces will be used as input to a structure model of the telescope generated by **SMI**.

The *seismic motion of the ground* is simulated by measured PSDs of typical ground acceleration at Cerro Paranal. The ground acceleration PSD is converted into a random time series serving as further input to the structure model —in addition to the dynamic wind forces.

Atmospheric turbulence creates temporal and spatial fluctuations of the phase of the electric field of each interferometer beam. In current version the three lowest order modes (piston and tip/tilt) are computed using analytical expressions of their PSDs based on Kolmogoroff statistics. The correlation between atmospheric piston on two telescope apertures separated by a given baseline is simulated. The PSDs are converted into random time series. Higher-order modes are represented by time-varying Zernike coefficients. These are extracted from moving phase screens independently computed for each aperture. Piston is (partially) corrected by the fringe tracking loop. Tip/tilt is compensated by the fast tip/tilt control loop. The higher-order modes remain uncorrected (assuming the absence of an adaptive optics system) and are directly added to the electric field distributions at the exit pupils in the beam combination laboratory.

3.2.3. The representation of signals

In the dynamic simulation, each interferometer beam is characterized by its *beam characteristics state vector* $\mathbf{z} = (\delta v,\ \delta w,\ \delta R,\ \delta\xi_1,\ \ldots,\ \delta\xi_N)^T$. The components δv and δw are the deviations of the exit pupil center from its static position (measured in the $(v,\ w)$-plane in the beam combination laboratory, see Figure 1). The dynamic wavefront aberrations are encoded in a set of Zernike polynomials with coefficients ξ_i $(i = 1 \ldots N;\ 3 \leq N \leq 37)$ (see 2). The Zernike decomposition uses a normalization radius whose deviation from the static value is given by δR.

The state vector $\mathbf{z}$ has the size $(3 + N) \times 1$, i.e. 40×1 for $N = 37$. This is reflected in the labels attached to the signal flow lines in the Simulink block diagram of the single interferometer arm shown in Figure 5. The block diagrams showing the top-level architecture (Figure 3) and the fringe tracking loop (Figure 4) represent an array configuration with two apertures. Their beam characteristics signal flow lines (label "80") hold two vectors $\mathbf{z}_1$ and $\mathbf{z}_2$ related to the two interferometric beams.

The disturbance signal vector entering the subsystem model of a single UT arm (Figure 5) is of size $(7+N) \times 1$ $(= 44 \times 1$ for $N = 37)$. The label "4{44}" in Figure 5 indicates that the disturbance vector is divided into four groups: (i) wind load (4 components corresponding to the four above mentioned load cases, see Section 3.2.2), (ii) seismic noise (3 components representing the accelerations along u, v and w-directions), (iii) atmospheric piston and tip/tilt (3 components), and (iv) higher-order modes of atmospheric turbulence $(37 - 3 = 34$ components). The telescope subsystem (block labelled "`Telescope`") contains an **SMI**-created structure model coupled to a **BeamWarrior**-created linear optical model. The output vector of the linear state-space structure model has the size 48×1 —holding 6 DOFs (translation and rotation) for each mirror M1 ... M8. It is passed as input to the optical model represented by a 40×48 sensitivity matrix. All control loops directly act on the beam characteristics vector $\mathbf{z}$. The fast tip/tilt loop additionally acts on a 2×1 vector $(\delta X, \delta Y)$ defining the deviation of the image position in the transmitted Coudé focus from its static value.

3.2.4. A simplified beam combiner model

The output of the integrated model is the time-dependent electric field in the VLTI exit pupils located in the beam combination laboratory. This location corresponds to the interface between the interferometer and the scientific instruments. The model output can serve as input to an instrument model. We have developed a simplified model of the test instrument VINCI currently operating with the VLTI.[6] It computes interference fringes assuming "pupil-plane" (i.e. coaxial) beam combination of two beams using a temporal optical pathlength modulation scheme. VINCI performs modal filtering using single-mode fibers to "clean" the wavefronts before

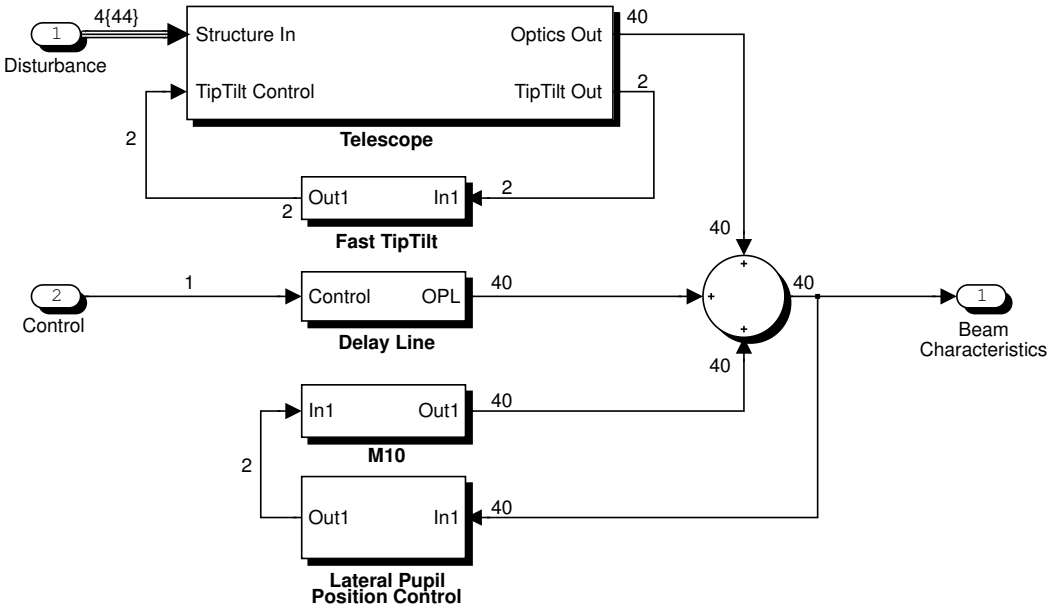

Figure 5. Subsystem model of a single interferometer arm (UT) with the main control loops

interferometric superposition. In this way spatially and temporarily varying wavefront aberrations across each beam are "translated" into temporal variations of optical power at the fiber output. In our model we simulate the effect of modal filtering by computing the *complex field coupling efficiency*[7]

$$\vec{\eta}_i^{Pol}(t) = \iint \mathbf{E}_i^{Pol}(\mathbf{x}, t) \cdot \Psi_{LP01}^*(\mathbf{x})\ dS \qquad (i = 1, 2, Pol = s, p). \tag{3}$$

where $\mathbf{E}_i^{Pol}(\mathbf{x}, t)$ is the time-dependent electric vector field in the exit pupil for both star polarizations ($Pol = s, p$) (see Equation 1). The field distribution $\Psi_{LP01}(\mathbf{x})$ represents the Gaussian approximation of the fundamental mode ($LP01$) of the fiber —back-propagated from the fiber input to the VLTI exit pupil plane:

$$\Psi_{LP01}(\mathbf{x}) = \sqrt{\frac{2}{\pi}} \cdot \frac{1}{\tilde{\omega}_0} \cdot \exp(-\frac{|\mathbf{x}|^2}{\tilde{\omega}_0^2}) \tag{4}$$

with $\tilde{\omega}_0 = \lambda f/(\pi\omega_0)$ where f is the focal length of the fiber injection optics and ω_0 is the mode field radius of the fundamental mode *in the fiber*. The vector $\mathbf{x}$ denotes a position in the VLTI exit pupil plane, i.e. $\mathbf{x} = (v, w)$, $|\mathbf{x}|^2 = v^2 + w^2$ (compare Figure 1). Both field distributions, $\mathbf{E}_i^{Pol}$ and Ψ_{LP01}, are normalized to unit power prior to integration. The integration is performed over the entrance aperture of the fiber injection optics. The coupling efficiency $\vec{\eta}_i^{Pol}$ is a vector with two elements for the two Cartesian components (v, w) of the electric field.[†]

Interference fringe scans are generated by modulating the optical pathlength in one arm (e.g. $i = 1$) with a sawtooth signal. The sampling frequency ("frame rate") is chosen such that a single fringe (corresponding to an OPD modulation range of one wavelength) is sampled at five points. After modal filtering, the fields of the two arms related to the *same* star polarization are superposed in a partial coherent way considering temporal coherence effects due to the finite spectral bandwidth of the source. This results in two interferograms for the two star polarizations $Pol = s, p$ which are then added on intensity-basis.

[†]The third component of the electric field along the optical axis (u) can be neglected since the wavefront is nearly planar.

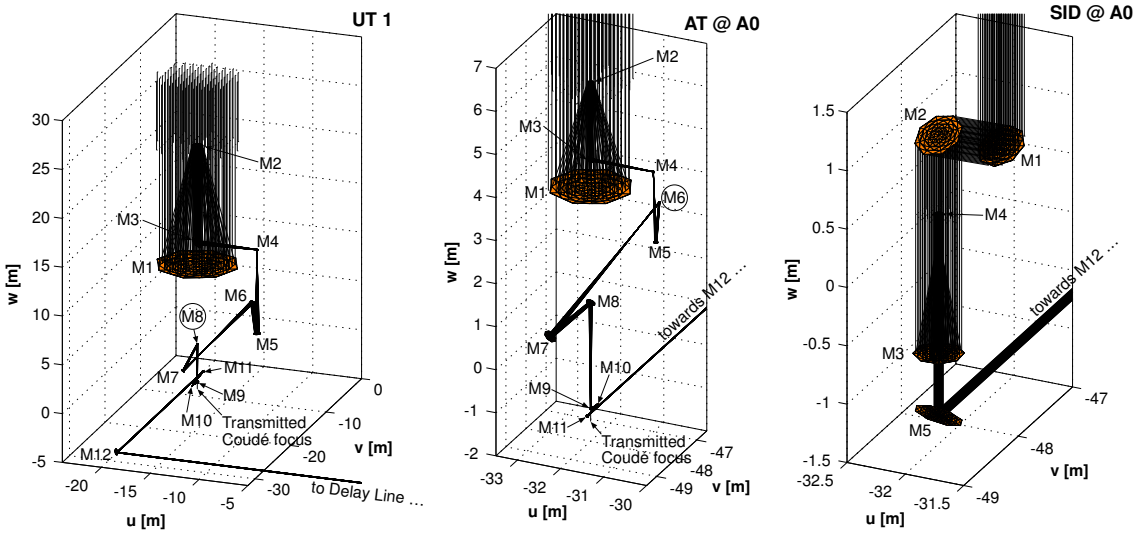

Figure 6. BeamWarrior models of the three types of VLTI telescopes (left to right): Unit Telescope (UT), Auxiliary Telescope (AT) and Siderostat (SID); the encircled mirror labels "M8" (UT) and "M6" (AT) indicate mirrors onto which a pupil (= image of aperture stop M2) is located. For the UT and AT, an image of the star is located in the transmitted Coudé focus below the dichroic mirror M9 and in the reflected Coudé focus on the field mirror M10. Note the different scales of the three plots.

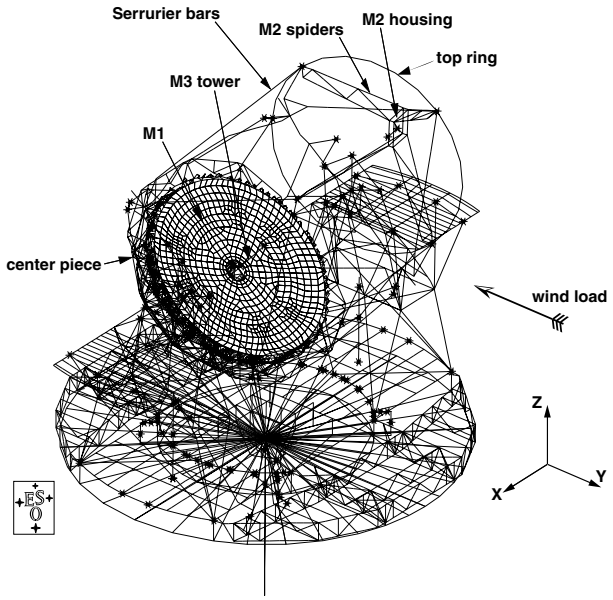

Figure 7. FEM model (6378 nodes) of the UT used within the VLTI integrated model; The model was set up in ANSYS. The telescope points to an altitude angle of 50 degrees. The total wind load is divided into four groups with independent force fields (see Section 3.2.2).

3.3. Results

Figure 8 shows simulated temporal interference fringe scans for a baseline of 56 m between two SIDs located at stations G0 and I1. The point source is observed in K-band ($\lambda = 2.2\ \mu m, \Delta\lambda = 400\ nm$). A "batch" of five consecutive scans is computed for two cases: with and without the fringe tracking loop activated. Each scan consists of 512 intensity values (so-called "frames") sampled at a frequency ("frame rate") of 800 Hz. The peak-to-valley amplitude of the OPD modulation is 225 μm corresponding to 18 times the coherence length and a "fringe speed" of 352 $\mu m\ sec^{-1}$ (i.e. 5 frames per fringe).

As stated in Section 3.2.2 the only disturbance taken into account for SID is atmospheric turbulence. In our simulation, only the three lowest-order modes (piston and tip/tilt) are active. The Fried parameter r_0 and mean wind speed $\overline{v}$ are set to the following values: $r_0 = 1.1\ m$ (corresponding to a seeing of 0.55 $arcsec$ at $\lambda = 500\ nm$) , $\overline{v} = 11.6\ m\ sec^{-1}$ (corresponding to a coherence time t_0 of 5 $msec$ at $\lambda = 500\ nm$). Since the aperture of a SID (40 cm) is small compared to r_0 higher-order modes of atmospheric turbulence would show no significant impact on the fringes.

For the simulation the mode field radius is set to $\omega_0 = 4.1\ \mu m$ —corresponding to a maximum coupling efficiency for a flat-top electric field distribution of diameter 18 mm into the Gaussian mode of a single-mode fiber.[‡]

Comparing the two batches in Figure 8 shows the effect of the fringe tracking control loop on the repeatability of the "white light fringe" position (i.e. maximum of coherence envelope) within different scans. The case "without fringe tracking" (left column in Figure 8) rather corresponds to the current situation of VLTI operations where no fast fringe tracking control loop is present.

It is pointed out that the VLTI integrated model recently has reached the state to produce its first results. The next steps will concentrate on validation of these results by comparing them with measured data. For this purpose it is planned to store the simulated VINCI fringes in the same format (FITS binary table) as used by the "real" VINCI. This will allow to process the data with the VINCI Data Reduction Software (DRS) which computes calibrated visibilities.[6]

4. SUMMARY AND OUTLOOK

A modular and flexible approach to integrated modeling of astronomical telescopes and stellar interferometers has been presented by showing its application to the VLTI. The approach is based on the optical modeling tool **BeamWarrior** and the structural modeling tool **SMI** which are used to create dynamic models of technical subsystems (e.g. telescope, delay line) in the optical and mechanical disciplines, respectively. The subsystem models are well suited for integration into a dynamic control loop model implemented in Matlab/Simulink.

The concept has been applied to the VLTI resulting in an integrated model of the interferometer covering the main control loops and most critical disturbances. The highly modular architectural design of the model reflects the VLTI hardware with its subsystems as installed on Cerro Paranal. Supplemented by a simplified model of the VINCI beam combiner, the model computes temporal interference fringes for observation of a point source.

Future work will concentrate on validation of the model results by comparison with measured VLTI/VINCI data. This implies adaption of the output data format to the FITS binary table format as used by the "real" VINCI. As additional disturbance source, we intend to include air-turbulence in the Delay Line tunnel for which measured data (lateral pupil motion, piston and tip/tilt) are available.

The VLTI integrated model can be regarded as a "precursor" model for future telescope or interferometer projects. Besides its "demonstrator role", it will also serve for practical applications. An important example is prediction of the dynamic VLTI output performance at interface-level to future scientific instruments. Being able to deliver synthetic data it can also be employed during the development or upgrade of data reduction software.

[‡]The optimum field radius ω_0 is given by $1.12 \times \lambda \times f \times \pi^{-1} \times R^{-1}$ with $f = 46.8\ mm$ (VINCI injection optics), $R = 9\ mm$, $\lambda = 2.2\ \mu m$. This formula neglects the central obscuration in the pupil for which the optimum radius would be slightly smaller.[8]

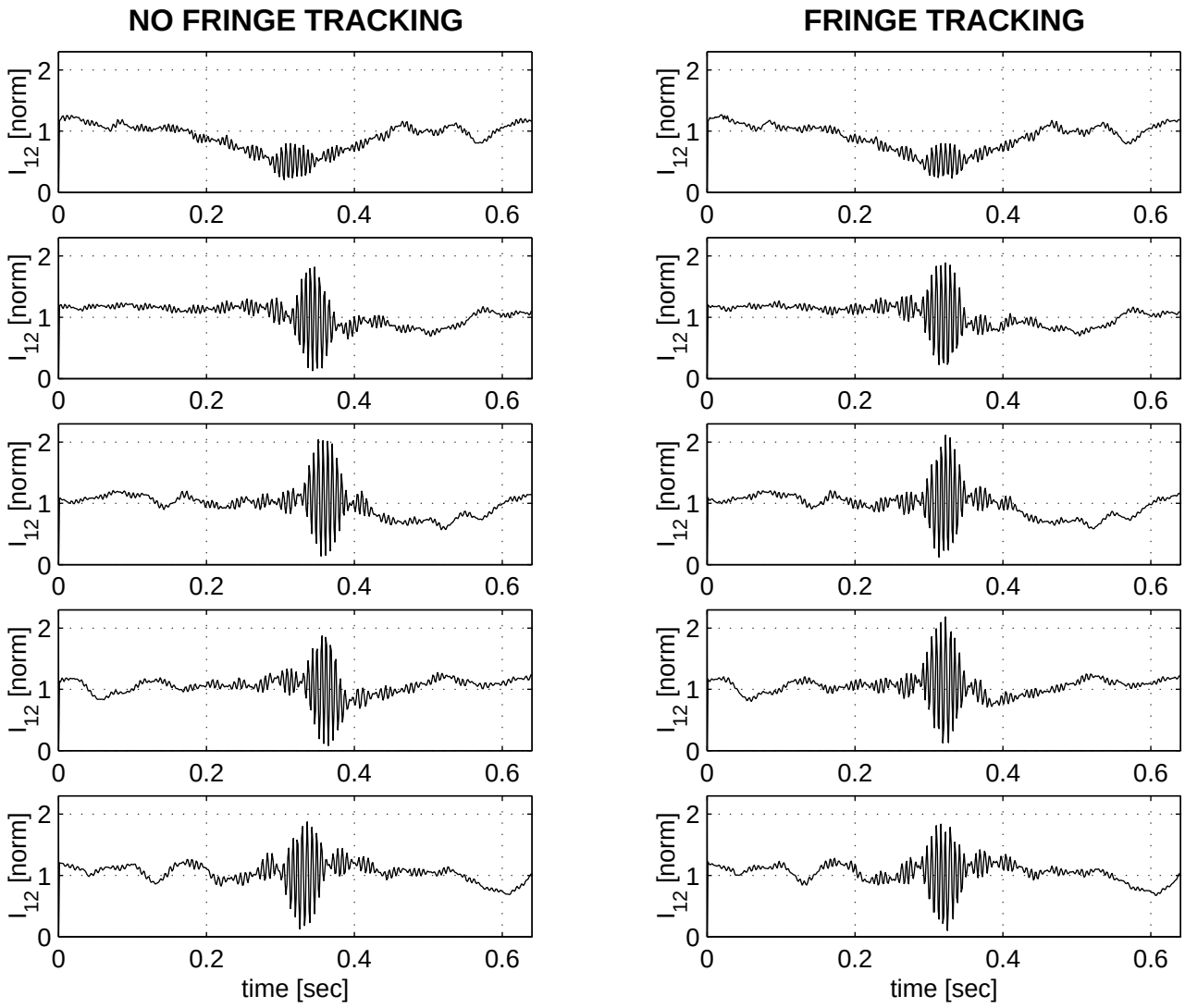

Figure 8. Batch of five simulated VINCI scans (K-band) for the baseline between two SIDs located at stations G0 and I1, respectively; the intensity values I_{12} are normalized to the mean value of the respective batch; *left:* no fringe tracking control loop; *right:* with active fringe tracking (FINITO & OPDC & DL); Frame rate = 800 Hz, 512 frames per scan; OPD modulation amplitude (peak-to-valley over one scan) = 225 μm

ACKNOWLEDGMENTS

The authors wish to thank Alberto Gennai and Serge Menardi (ESO VLTI Group) for providing Matlab models of the Fringe Sensor Unit, Delay Line and OPD Controller. The contribution of phase screens by Rodolphe Conan (ESO Adaptive Optics Group) is gratefully acknowledged. Thanks to Alexis Huxley (ESO VLTI Group) for critically reviewing the manuscript.

REFERENCES

1. M. Schoeller, R. Wilhelm, and B. Koehler, "Modeling the imaging process in optical stellar interferometers," *Astron. & Astrophys. Suppl. Ser.* **144**, pp. 541–552, 2000.
2. R. Wilhelm, *Novel numerical model for dynamic simulation of optical stellar interferometers*, Logos Verlag (also: Technische Universitaet Berlin, Dissertation), Berlin, 2000.
3. R. Wilhelm, "Comparing geometrical and wave optical algorithms of a novel propagation code applied to the VLTI," in *Wave-Optical System Engineering*, F. Wyrowski, ed., *Proc. SPIE* **4436**, pp. 89–100, 2001.
4. M. Mueller and H. Baier, "SMI —a structural dynamics toolbox for integrated modeling," in *Workshop on Integrated Modeling of Telescopes*, T. Andersen, ed., *Proc. SPIE*, to be published 2002.
5. A. Glindemann, "Very Large Telescope Interferometer: a status report," in *Interferometry for Optical Astronomy II*, W. A. Traub, ed., *Proc. SPIE* **4838**, (these proceedings) 2002.
6. P. Kervella, "VINCI, the VLTI Commissioning Instrument: status after one year of operations at Paranal," in *Interferometry for Optical Astronomy II*, W. A. Traub, ed., *Proc. SPIE* **4838**, (these proceedings) 2002.
7. O. Wallner, *Private communication*, Technische Universitaet Wien, 2002.
8. C. Ruilier, "A study of degraded light coupling into single-mode fibers," in *Astronomical Interferometry*, R. D. Reasenberg, ed., *Proc. SPIE* **3350**, pp. 319–329, 1998.